Glycoconj J (2007) 24:231–241
DOI 10.1007/s10719-007-9030-7

Changes in GM1 ganglioside content and localization in cholestatic rat liver

Marie Jirkovská · Filip Majer · Jaroslava Šmídová · Jan Stříteský · Gouse Mohiddin Shaik · Petr Dráber · Libor Vítek · Zdeněk Mareček · František Šmíd

Received: 7 August 2006 / Revised: 26 January 2007 / Accepted: 2 February 2007 / Published online: 27 February 2007

Abstract (Glyco)sphingolipids (GSL) are believed to protect the cell against harmful environmental factors by increasing the rigidity of plasma membrane. Marked decrease of membrane fluidity in cholestatic hepatocytes was described but the role of GSL therein has not been investigated so far. In this study, localization in hepatocytes of a representative of GSL, the GM1 ganglioside, was compared between of rats with cholestasis induced by 17α-ethinylestradiol (EE) and vehicle propanediol treated or untreated animals. GM1 was monitored by histochemical reaction employing cholera toxin B-subunit. Our findings in normal rat liver tissue showed that GM1 was localized in sinusoidal and canalicular hepatocyte membranes in both peripheral and intermediate zones of the hepatic lobules, and was nearly absent in central zones. On the contrary, in EE-treated animals GM1 was also expressed in central lobular zones. Moreover, detailed densitometry analysis at high magnification showed greater difference of GM1 expression between sinusoidal surface areas and areas of adjacent cytoplasm, caused as well by increased sinusoidal staining in central lobular zone as by decreased staining in cytoplasm in peripheral zone. These differences correlated with serum bile acids as documented by linear regression analyses. Both GM1 content and mRNA corresponding to GM1-synthase remained unchanged in livers; the enhanced expression of GM1 at sinusoidal membrane thus seems to be due to re-distribution of cellular GM1 at limited biosynthesis and could be responsible for protection of hepatocytes against harmful effects of bile acids accumulated during cholestasis.

Keywords Cholestasis · Ethinylestradiol · Hepatocyte · Cholera toxin · Gangliosides

Abbreviations

ALP	alkaline phosphatase
BSA	bovine serum albumin
EE	17α-ethinylestradiol
PD	1,2-propanediol
GSL	glycosphingolipids
PBS	phosphate buffer saline
TBA	total bile acids

Ganglioside symbols, according to Svennerholm [26, 27], with IUPAC-IUB [28] nomenclature in parentheses

GM3	(II^3NeuAc-LacCer)
GM2	(II^3NeuAc-GgOse$_3$Cer)

M. Jirkovská · J. Šmídová
Institute of Histology and Embryology,
Prague, Czech Republic

F. Majer · L. Vítek · F. Šmíd (✉)
Institute of Clinical Biochemistry and Laboratory Diagnostics,
1st Faculty of Medicine, Charles University,
U Nemocnice 2, 128 08 Prague 2, Czech Republic
e-mail: smid@cesnet.cz

L. Vítek
4th Department of Internal Medicine,
Prague, Czech Republic

Z. Mareček
General Military Hospital, Prague, Czech Republic

J. Stříteský
Institute of Pathology, 1st Medical Faculty,
Charles University, Prague 2, Czech Republic

G. M. Shaik · P. Dráber
Department of Signal Transduction, Institute of Molecular Genetics, Academy of Sciences of the Czech Republic,
Prague 4, Czech Republic

GM1 (II^3NeuAc-GgOse$_4$Cer)
GD3 (II^3(NeuAc)$_2$-Lac-Cer)
GD2 (II^3(NeuAc)$_2$-GgOse$_3$Cer)
GD1a (IV^3NeuAc,II^3NeuAcGgOse$_4$Cer)
GD1b (II^3(NeuAc)$_2$-GgOse$_4$Cer)
GT1b (IV^3NeuAc,II^3(NeuAc)$_2$-GgOse$_4$Cer)

Introduction

Plasma membrane (glyco)sphingolipids (GSL) are generally believed to protect cells against harmful environmental factors by forming a mechanically stable and chemically resistant outer leaflet of the lipid bilayer. Apart from this function complex GSL are assumed to self-aggregate and form less liquid sphingolipid/cholesterol based plasma membrane microdomains, also called "lipid rafts" which are likely to play an important role in signal transduction and cell–cell recognition [1, 2].

The membrane of polarized epithelial cells consists of functionally different apical and basolateral domains displaying specific protein and lipid composition. These proteins and lipids are sorted in the trans-Golgi network and then directly transported to the apical membrane [1]. Some evidence for direct transport of proteins into the plasma membrane in hepatocytes also exists, but numerous apical membrane proteins are indirectly sorted and lipid rafts seems to be instrumental in targeting of some apical proteins [3].

Like proteins, lipids also show polarized distribution as evidenced by studies with hepatocyte-derived HEP-G2 cells incubated with fluorescent dye-labeled glucosylceramide and sphingomyelin [4]. In these experiments, the fluorescent analog of glucosylceramide displayed a preferential localization in canalicular membrane while the fluorescent analog of sphingomyelin was sorted into basolateral pole via the reverse transcytotic route [4]. Nevertheless, the distribution of GSL in the canalicular and basolateral membranes of hepatocytes has not been investigated *in situ*.

Experimental studies showed that administration of synthetic estrogen 17α-ethinylestradiol (EE) resulted in reversible intrahepatic cholestasis [5]. However, its pathogenesis still remains enigmatic. In this connection it should be noted, that it was described more than two decades ago that erythrocytes from patients with cholestasis exhibited a decreased membrane fluidity [6]. Next, Smith and Gordon analyzed rat livers with EE-induced cholestasis and found an increase in cholesterol ester and sphingomyelin content, as well as an increase in the cholesterol/phospholipid ratio, but an unaltered fatty acids composition [7]. The decreased fluidity persisted not only in liposomes prepared from total liver extract of treated rats but also in liposomes of the phospholipid (sphingomyelin) fraction which was prepared by precipitation with cold acetone. GSL were no doubt present in this phospholipid/sphingomyelin fraction, but they were not analyzed. Furthermore, Rosario et al. [8] examined the effect of EE administration on protein and lipid composition as well as membrane fluidity using purified sinusoidal and canalicular membrane fractions and found that EE administration selectively decreased sinusoidal membrane fluidity. Lipid analyses showed only minor changes in phospholipid/sphingomyelin/phosphatidylcholine ratio, cholesterol/phospholipid ratio and fatty acid distribution, which could not explain a decrease of membrane fluidity. Again, complex GSL were not analyzed. In addition, altered membrane fluidity was also described in cholestasis induced with lithocholate [9], as well as bile duct ligation, or phalloidin infusion [10, 11].

In our previous experiments we examined the composition of gangliosides by thin layer chromatography (TLC) in extracts from livers of rats with EE-induced cholestasis or control animals, and found that content of GM1 ganglioside was not changed, GD1a increased slightly whereas GD3, GD1b and GT1b increased strongly. Total lipid sialic acid was almost twice as high as the control level (p=0.002) [12].

The aim of this study was to determine changes in topography of ganglioside GM1 in EE-induced cholestatic rat liver, as detected by histochemistry with GM1-specific probe, cholera toxin B-subunit.

Materials and methods

Animals and treatments, induction of cholestasis

Female Wistar rats were housed under controlled temperature and a natural light–dark cycle. The animals had free access to food and water throughout the experiments and were fasted the night before experimentation. All aspects of the study met the accepted criteria of experimental use of laboratory animals and all protocols were approved by the Animal Research Committee of the 1st Medical Faculty, Charles University of Prague.

Cholestasis was induced in the experimental group (n= 11) by subcutaneous injections of EE (Sigma, St Louis, MO, USA) in a dose 5 mg/kg b.wt. dissolved in 0.2 ml of 1,2-propanediol (PD) (Fluka, Switzerland) applied daily for 18 days.

The control group of animals consisted of a subgroup (n= 7) without any treatment and a subgroup (n=8) treated with 0.2 ml of PD daily.

After laparotomy under ether anaesthesia, the inferior vena cava was cannulated, blood samples were collected and livers were flushed blood-free with heparin (100.000 IU/l) in saline for 2 min and weighed. Pieces of liver tissues were

appropriately processed for further biochemical and histochemical analyses (see below). For quantitative histochemical analysis of GM1 ganglioside, the liver specimens were collected using systematic uniform random sampling method.

Analysis of serum markers of cholestasis

In order to determine the degree of cholestasis and liver injury, the following serum levels were assessed: total bile acids (TBA), total bilirubin, alkaline phosphatase (ALP), aspartate aminotransferase (AST), alanine aminotransferase (ALT). TBA were determined enzymatically (spectrophotometric kit BI-1605, Randox, UK), while all other markers were quantified on an automatic analyzer (model 717; Hitachi, Tokyo, Japan). In detail, bilirubin was analyzed by the diazo reaction, the activities of serum transaminases and ALP were determined enzymatically using routine commercial chemicals.

Isolation and TLC analysis of liver gangliosides

Gangliosides were isolated using the procedure previously described [12] and finally purified on a small silica gel column [13]. Gangliosides were separated in a solvent system (chloroform/methanol/0.2% aqueous $CaCl_2$, 55/45/10 v/v/v) and detected with resorcinol-HCl reagent.

Light microscopy

Small tissue blocks (about 1 mm^3) were fixed in 4% paraformaldehyde in Na-cacodylate buffer (pH 7.4) for 2 h, dehydrated subsequently in graded methanol at 4 °C and −20°C, and embedded in LR Gold resin (Sigma). Polymerization was performed under UV light at −25°C overnight. Semi-thin sections were cut, stained with toluidine blue and examined for autofluorescence of pigment granules.

Alkaline phosphatase histochemistry

Tissue specimens were rapidly frozen in liquid nitrogen. The catalytic activity of ALP was demonstrated in thin 6 μm cryostat sections using simultaneous azo-coupling method [14]. Control and experimental sections were incubated together for 150 min at room temperature, counterstained with Mayer´s hematoxylin and mounted in glycerine jelly.

GM1 histochemistry

Frozen 6 μm sections were fixed first in dry cold acetone (−20°C) for 2 min and then in 4% freshly prepared paraformaldehyde for 20 min. Endogenous peroxidase activity was blocked by incubation for 15 min in PBS supplemented by 1% H_2O_2 and 0.1% dissolved sodium azide.

Endogenous biotin was blocked by means of the blocking kit (DakoCytomation, Denmark). In order to block nonspecific binding, sections were treated with 3% BSA in PBS for 15 min. Cholera toxin was used for GM1 ganglioside detection [15]. Sections were incubated for 60 min at room temperature with biotinylated cholera toxin-B-subunit (List Biological Laboratories, USA) diluted 1:250 in PBS plus 3% BSA. After washing in PBS, the sections were labeled with Streptavidin-peroxidase polymer Ultrasensitive (Sigma, St. Louis, USA) diluted 1:400 in PBS containing 0.05% Tween 20 at room temperature for 60 min. Peroxidase activity was visualized with diaminobenzidine. Sections were counterstained with Mayer´s hematoxylin and mounted in glycerine jelly.

Two control tests were included in each series. First, fixed sections were extracted with chloroform–methanol mixture 2:1 at room temperature for 30 min, followed by histochemical staining. Second, the cholera toxin B-subunit was omitted in negative control tests.

Quantiative study on the distribution of GM1 ganglioside in the hepatic lobule

In this study, 11 animals from EE-treated and seven from untreated control group were used. From each liver, six pieces of randomly sampled tissue blocks were taken. One frozen 6 μm thick section was used from each block, and all sections were stained simultaneously using the above described histochemical reaction. The hematoxylin counterstaining was omitted.

The images of whole sections were photographed at the objective magnification 5× (NA=0.12) and stored using the IM 500 Image Manager (Leica). The quantity of reaction product was determined as mean optical brightness of marked area using the image analysis program ACC 6.0 (SOFO, Czech Republic). Two ways were used for the quantification. First, whole section was marked and its mean optical brightness was evaluated. Second, areas of liver parenchyma in peripheral (periportal; zone I) intermediate (zone II) and central (zone III) zones of hepatic lobules were marked and their mean optical brightness was determined separately.

Densitometric analysis of the amount of GM1 ganglioside in areas of sinusoidal membrane and of adjacent cytoplasm

Ten animals from EE-treated, eight animals from PD and six animals from the control group were taken to this analysis. Six liver specimens were used from each animal. One section from each specimen was used for GM1 ganglioside detection with cholera toxin B-subunit histochemical procedure as

described above. On each section, four hepatic lobules with clearly discernible central vein were selected. In each lobule, one measuring frame in central lobular zone III and one measuring frame in corresponding peripheral lobular zone I were selected for analysis. In each frame, 15 areas of sinusoidal surface and 15 areas of adjacent hepatocyte cytoplasm were selected by the stratified random sampling method [16] and marked out. The reaction product was quantified as mean optical density of analyzed areas as determined by the densitometric program CUE 2 (Olympus) at objective magnification 40× (NA=0.7).

RNA extraction, cDNA synthesis and quantitative real-time PCR

RNA was extracted from liver cells of control or EE-treated animals using RNA Blue reagent (Top-Bio, Czech Republic). Purity and quantity of RNA was checked by Nanodrop spectrophotometer (NanoDrop Technologies, USA). Single-strand cDNA synthesis was performed using MMLV reverse transcriptase (Invitrogen, USA) according to manufacturer's instructions; a mixture of 10 μg of isolated RNA and 50 ng of random hexamers was used per reaction. Quantitative real-time PCR was performed using Mastercycler ep realplex (Eppendorf, Germany). Eight-fold diluted single-strand cDNA was used as template and mixed at 1:1 (vol:vol) with qPCR 2× SYBR green master mix containing 20 mM Tris-HCl, pH 8.8, 100 mM KCl, 0.2% Triton X-100, 3 mM $MgCl_2$, 400 μM dATP, 400 μM dTTP, 400 μM dGTP, 400 μM dCTP, 50 U/ml Taq DNA polymerase, SYBR green and primers. Primers were added to the final concentration of 0.25 μM. The following primers were used: actin forward: 5′ ACTCTTC CAGCCTTCCTTCC 3′; actin reverse: 5′ ATCTCCTTCTG CATCCTGTC 3′; GalTII (galactosyl(Gal)-transferase II, GM1-synthase) forward: 5′ AACGCCATTCGGGGATCTT 3′; GalTII reverse: 5′ CTCTGAGGCCAGGTCAGCAAA 3′; SATII (sialyl(NeuAc)-transferase II, GD3-synthase) forward: 5′ GTAATGAAAGCCTTAAGCACAGC 3′; SATII reverse: 5′ CTTCTCTGCATCCAGGAACTTT 3′. To ensure that correct DNA fragments were amplified in PCR, a melting curve of PCR products was obtained. Furthermore, the size of all PCR products was controlled by electrophoresis. The final real-time-PCR data were expressed as the C_T of GalTII and SATII normalized with the C_T of β-actin of each sample.

Statistical analysis

Data are presented as mean ± SD, or median and 25–75% range. The statistical significance of differences between variables was evaluated by *t* test or Mann-Whitney Rank Sum test in cases where data were not normally distributed. Histochemical data are presented as the mean ± SD of optical brightness, or differences between the optical brightness in peripheral and central zones of hepatic lobules, or the ratios of optical densities measured in sinusoidal membranes and hepatocyte cytoplasm (sin/cyt) in peripheral and central lobular zones. Differences with $p < 0.05$ were considered significant. The most significant results were correlated with the serum TBA concentrations using linear regression analysis. All calculations were performed using software EpiInfo 3.2.2 (Centers for Disease Control and Prevention, Atlanta, Georgia, USA).

Results

Biochemical analyses

Administration of EE resulted in severe cholestatic liver injury as evidenced by significant elevation of serum TBA and bilirubin (Table 1). Controls treated with similar volumes of PD, a vehicle for EE, showed no significant change in TBA and bilirubin values (not shown).

Light microscopy

Unlike the findings characteristic for control animals (Fig. 1a), morphological signs of cholestasis were found in the liver of EE-treated rats, even though individual liver samples differed in the degree of pathological changes. More or less conspicuous degree of feathery degeneration of hepatocytes occurred mainly in peripheral areas of lobules, though it was found occasionally in hepatocytes of all lobular zones (Fig. 1b, d). Liver samples of EE-treated animals displayed also variable amounts of intracellular bile pigments, while no pigment depositions were found in bile canaliculi (Fig. 1c). In some cases, fatty degeneration with numerous lipid droplets in hepatocytes was observable particularly in the zone I and zone II of the lobule (Fig. 1b). Liver cells displaying features of apoptosis or necrosis were evenly spread throughout the liver parenchyma (Fig. 1d).

Alkaline phosphatase histochemistry

EE-induced cholestasis was also reflected in ALP catalytic histochemical analysis. In the control group, ALP was confined just to the canalicular membrane of hepatocytes in peripheral zones (zone I) of hepatic lobules and the enzyme activity expressed by the amount of reaction product was very low (Fig. 1e). The sections from EE-influenced liver specimens showed a markedly higher amount of the reaction product lining the canalicular and basolateral hepatocyte membranes in all zones of hepatic lobules. Only those parts of hepatocyte membrane directly adjacent to blood sinusoids displayed no enzymatic activity (Fig. 1f).

Table 1 Serum levels of cholestatic markers in control and experimental groups

	Controls (n=7)	EE-treated rats (n=11)	p-value
Weight of rats [g]	296±26	219±34	0.00001
Weight of liver [g]	10.7 (9.6–11.2)	9.6 (8.6–11.9)	0.63
TBA [μmol/l]	45 (21–53)	382 (256–619)	0.00001
Bilirubin [μmol/l]	2.0 (1.9–2.4)	7.5 (5.5–27.8)	0.00001
ALT [μkat/l]	0.81 (0.75–1.04)	0.92 (0.81–1.20)	0.22
AST [μkat/l]	1.28 (1.17–1.61)	1.18 (1.00–1.77)	0.76
ALP [μkat/l]	2.12 (1.68–2.44)	2.42 (1.78–3.13)	0.38

Data are presented as mean ± SD, or median (25–75%) when not normally distributed

GM1 histochemistry

In the liver specimens of all control animals, a small amount of reaction product of GM1 ganglioside histochemistry was distributed on both the sinusoidal and canalicular membranes except for the central lobular zone (zone III), where almost no reaction occurred (Fig. 2a). In all EE-treated animals, the GM1 ganglioside was nearly uniformly distributed in all lobular zones from the portal areas up to the central veins (Fig. 2b). Sinusoidal surfaces of hepatocytes were conspicuously lined with the reaction product, whereas the reaction on canalicular surfaces was rather weak. Both control experiments in which either the GM1 was extracted or the cholera toxin was omitted gave negative results.

Quantiative study on the distribution of GM1 ganglioside in hepatic lobule

The distribution pattern of GM1 ganglioside in liver sections is demonstrated under low microscopic magnification (Fig. 3a, b). The amount of GM1 ganglioside expressed as

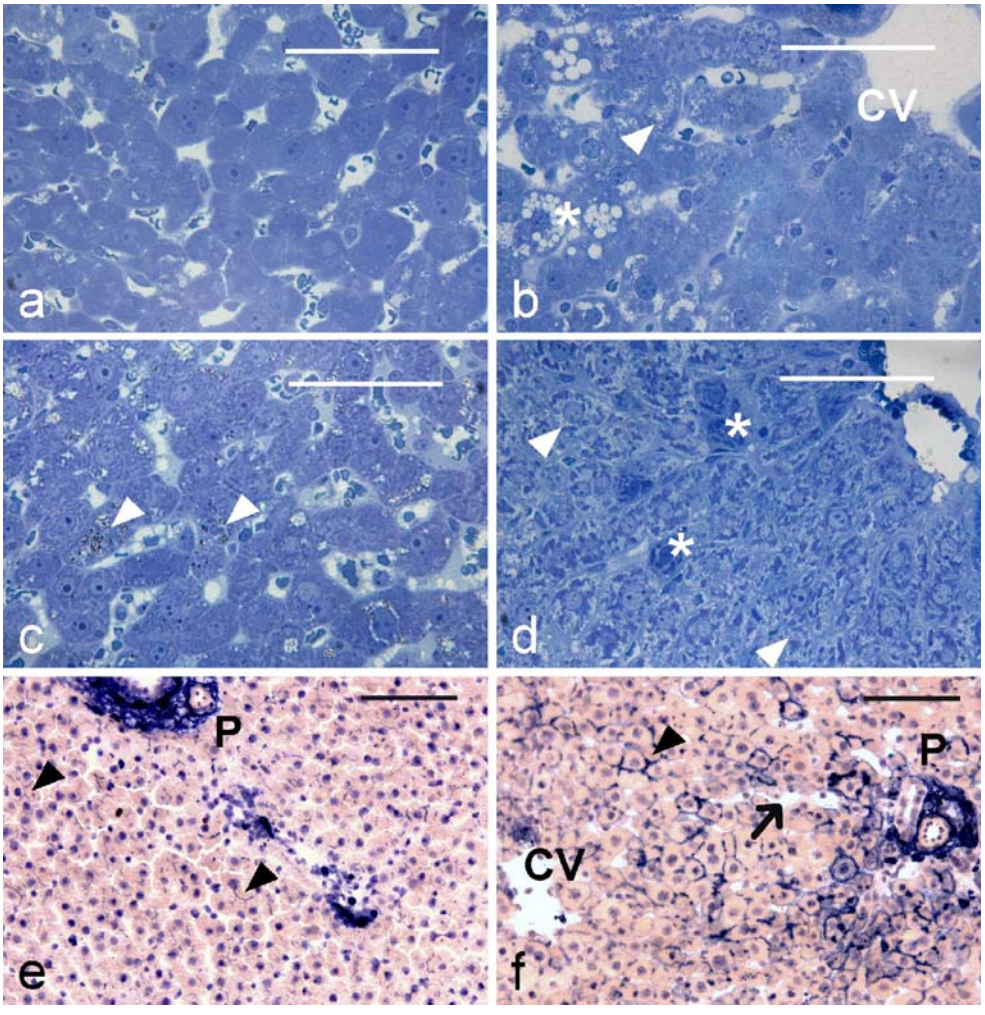

Fig. 1 Histopathological analysis of cholestatic rat livers. Light microscopy of the liver tissue of control and EE-treated animals. **a** Normal liver morphology, **b**,**c**, **d** EE-treated animals stained with toluidine blue. Pathological changes of hepatocytes were classified as follows: **b** steatosis (*) and some degree of feathery degeneration (*arrowhead*) in the central lobular zone **c** abundant intracellular localization of bile pigments (*arrowheads*), as revealed by light refraction. The pigment granules displayed no autofluorescence; **d** massive feathery degeneration (*arrowheads*) of hepatocytes and sparsely spread cells displaying some features of apoptosis and necrosis (*); **e**, **f** ALP histochemistry of liver tissue in EE-treated and control animals. **e** Control liver shows only mild ALP activity on the canalicular hepatocyte membrane at the periphery of hepatic lobule (*arrowheads*). **f** Except for the sinusoidal pole of hepatocyte membrane (*arrow*), the EE-treated liver displays ALP activity in canalicular and basolateral hepatocyte membranes in all zones of hepatic lobules (*arrowhead*); p = portal area, cv = central vein, *bars*=100 μm

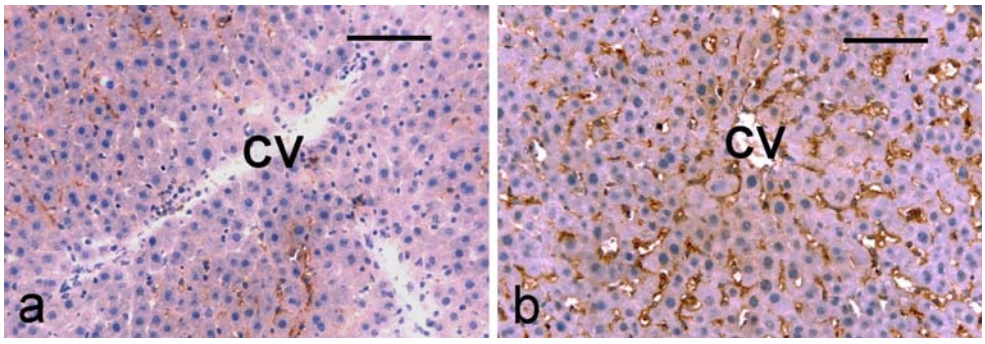

Fig. 2 Distribution of GM1 ganglioside. **a** In the control liver, a small amount of reaction product occurs in canalicular and sinusoidal hepatocyte membrane in peripheral and intermediate lobular zones (zone I and II) whereas the central zone is nearly free of it. **b** In the EE-treated liver, the reaction product is found in canalicular and sinusoidal hepatocyte membranes in all lobular zones; *cv* = central vein; *bars*=100 μm

optical brightness of whole sections showed no significant difference between EE-treated and control groups (Table 2). This finding corresponds to the insignificant difference of GM1 concentration determined by biochemical analysis. In contrast to the results obtained in whole sections, the differences of the GM1 content between peripheral and central lobular zones were significantly higher in controls (Table 2). The linear regression analysis demonstrated that the higher degree of cholestasis, measured by TBA concentration, correlated well with the lower difference of the GM1 content between lobular zone I and III.

Comparison of the amount of GM1 ganglioside in areas of sinusoidal membrane and of adjacent cytoplasm

The effect of EE on localization of GM1 was analyzed under high magnification. The results are summarized in Table 3.

Differences in GM1 staining between samples obtained from untreated and PD-treated animals

A possible influence of PD on GM1 staining was investigated by comparing the PD-treated animals and

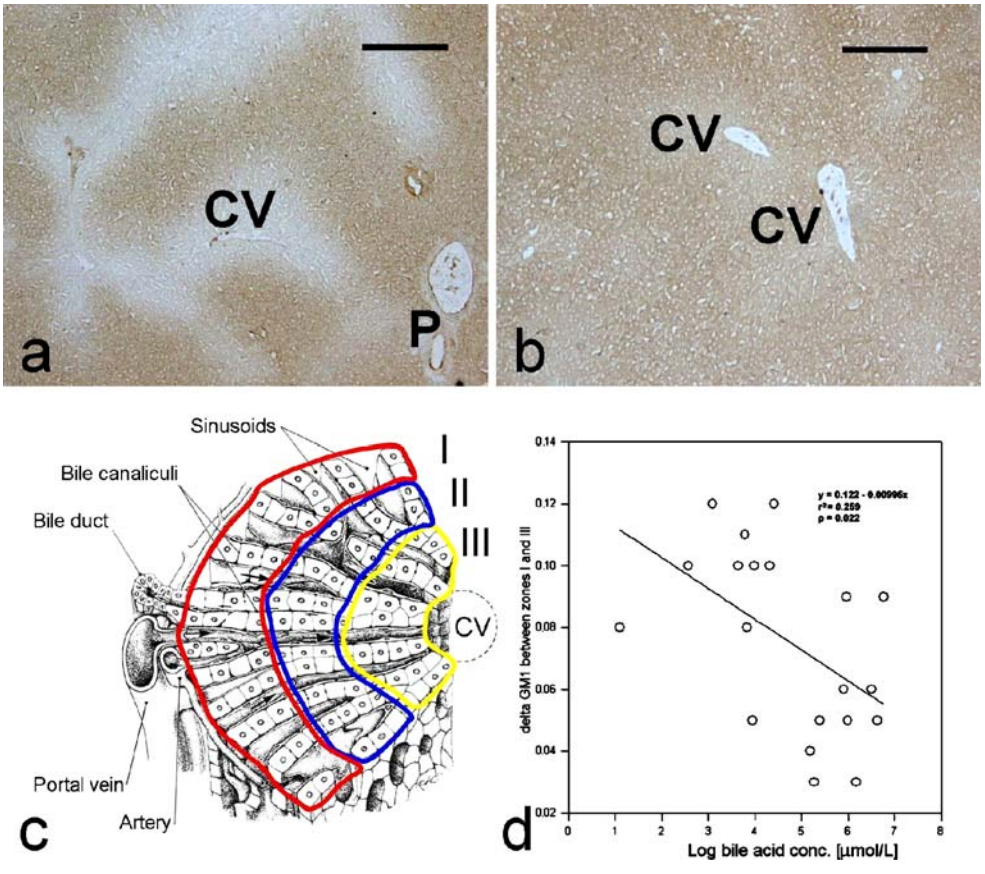

Fig. 3 Histochemical localization of GM1 ganglioside in rat liver as seen at low magnification. **a** In control liver, the reaction product occurs in lobular zones I and II and is nearly or completely absent in zone III. **b** In EE-treated liver, the difference in the amount of reaction product between peripheral and central areas of the lobule is hardly observable. *cv* = central vein, *p* = portal area; *bars*= 500 μm. **c** Schematic representation of the liver lobule with marked areas of measurement. *Red* = peripheral zone (zone I), *blue* = intermediate zone (zone II), *yellow* = central zone (zone III). **d** Linear regression analysis between serum TBA concentration and the difference in GM1 ganglioside content between lobular zones I and III

Table 2 Densitometric quantification of GM1 ganglioside in control and EE-treated livers

	Controls (n=7)	EE-treated rats (n=11)	p value
Mean optical brightness measured in whole sections	0.61±0.04	0.61±0.04	0.923
Differences of optical brightness between lobular zones I and III	0.097 (0.079–0.107)	0.055 (0.034–0.058)	0.0035

those without treatment. A slight increase of sinusoidal GM1 staining in zone III was observed (Table 3a; p=0.02). For this reason, PD-treated animals were used as controls in the study of EE influence on GM1 staining.

Significant changes were found neither in sinusoidal GM1 staining in zone I (Table 3b, p=0.57) nor in cytoplasm of both zones I and III (Table 3c, d). It should be noted that in untreated controls, significantly higher GM1 staining on sinusoidal surfaces was found in zone I compared to zone III (Table 3e, p=0.03).

The effect of EE-treatment on GM1 staining in areas of sinusoidal surface of central lobular zone III

Data in Table 3f show a significant increase of GM1 centrolobular sinusoidal surface areas of EE-treated rats when compared with those treated with PD (p=0.0002).

No significant difference in GM1 staining was found between EE- and PD-treated animals in cytoplasmic areas in zone III (Table 3g). Therefore, the increase of sin/cyt ratio seems to be due to increased sinusoidal staining in EE-treated animals (Table 3h, p=0.00002) at a stable level of staining in sub-sinusoidal areas of cytoplasm. Linear regression analysis confirmed that widening difference between sin and cyt staining correlated well (p=0.00001) with higher degree of cholestasis as indicated by higher serum TBA concentration (see Fig. 4d).

The effect of EE-treatment on GM1 staining in peripheral lobular zone I

Data presented in Table 3i show no significant difference in GM1 staining in sinusoidal surfaces areas in zone I between EE- and PD-treated animals (p=0.12). In contrast, the decrease of GM1 staining in the adjacent cytoplasmic area was found highly significant (Table 3j, p=0.0008). Consequently, the difference in ratios sin/cyt EE to sin/cyt PD is also highly significant (Table 3k, p=0.002). Examples of staining in cytoplasm of hepatocytes in periportal zone PD- and EE-treated livers are shown in Fig. 4b and c. Linear regression analysis confirmed that higher degree of cholestasis expressed as TBA concentration correlate with increasing difference between sin/cyt staining (Fig. 4e) in zone I. Finally, an increase of sinusoidal GM1 was found between zone III and zone I in both EE-treated (Table 3k, p=0.007) and PD-treated rats (Table 3m, p=0.0002).

Analysis of gangliosides and expression levels of mRNA of GM1-synthase and GD3-synthase

To clarify the biochemical basis of the observed differences between EE- and PD-treated animals we further analyzed the content of gangliosides in whole liver. Data presented in Fig. 5a shows a general scheme of ganglioside biosynthesis, consisting of *0, a, b* and *c* branch. TLC shows that in *a*-

Table 3 Results of densitometric quantification of GM1 ganglioside in areas of sinusoidal surface (sin) and of adjacent cytoplasm (cyt)

				Mean ± SD	Mean ± SD	p value
a	zone III sin PD	vs.	zone III sin C	0.184±0.012	0.164±0.015	0.02
b	zone I sin PD	vs.	zone I sin C	0.283±0.019	0.296±0.036	0.57
c	zone III cyt PD	vs.	zone III cyt C	0.141±0.013	0.135±0.012	0.47
d	zone I cyt PD	vs.	zone I cyt C	0.189±0.016	0.200±0.019	0.30
e	zone I sin C	vs.	zone III sin C	0.296±0.036	0.164±0.013	0.003
f	zone III sin EE	vs.	zone III sin PD	0.228±0.023	0.184±0.012	0.0002
g	zone III cyt EE	vs.	zone III cyt PD	0.138±0.020	0.141±0.014	0.75
h	zone III sin/cyt EE	vs.	zone III sin/cyt PD	1.675±0.144	1.313±0.108	0.00002
i	zone I sin EE	vs.	zone I sin PD	0.264±0.028	0.283±0.020	0.13
j	zone I cyt EE	vs.	zone I cyt PD	0.149±0.023	0.189±0.017	0.0008
k	zone I sin/cyt EE	vs.	zone I sin/cyt PD	1.803±0.204	1.511±0.074	0.002
l	zone I sin EE	vs.	zone III sin EE	0.264±0.028	0.228±0.023	0.007
m	zone I sin PD	vs.	zone III sin PD	0.283±0.019	0.184±0.011	0.0002

C = untreated controls.

branch of gangliosides, there is no significant difference in the amount of GM1 ganglioside and a slight increse in the amount of GD1a in EE-treated animals compared to PD-treated and untreated animals. There is a significant increase in GD3 and *b*-branch gangliosides. To determine whether there are any differences in the expression of enzymes involved in synthesis of GM1 or *b*-branch gangliosides, expression levels of mRNA for GalTII (galactosyl(Gal)-transferase II, GM1-synthase) and SATII (sialyl(NeuAc)-transferase II , GD3-synthase) were estimated using real-time PCR. Data presented in Fig. 5c reveal that there are no differences in the expression levels of GalTII mRNA and SATII mRNA between liver cells isolated from control or EE-treated animals.

Discussion

Several approaches may be used to study GSL in cholestatic liver membranes. Biochemical approach may be appropriate for analysis of GSL in membranes isolated by gradient untracentrifugation; however, it is difficult to obtain canalicular and basolateral membrane fractions in sufficient quantity and purity. Considering that ALP

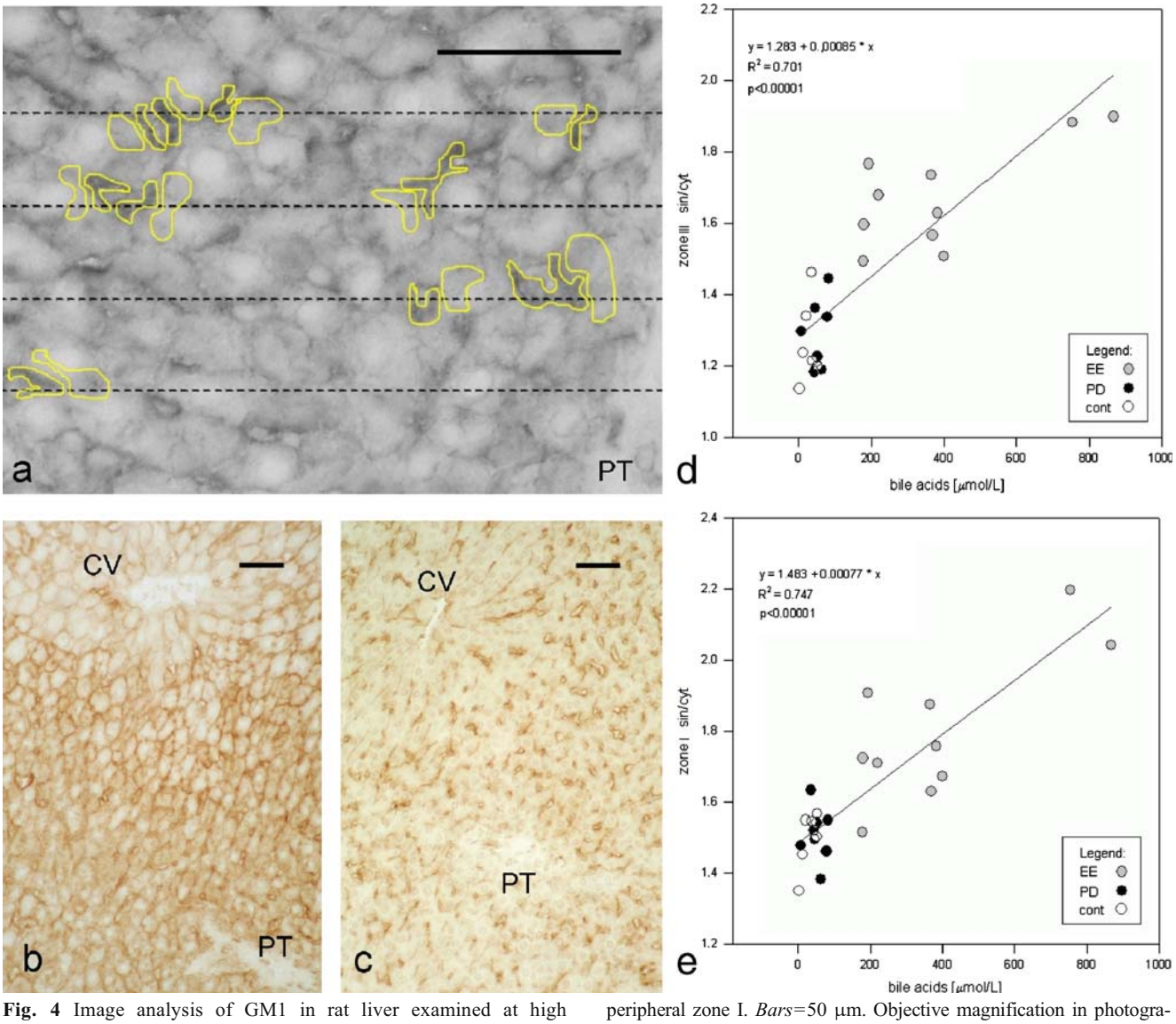

Fig. 4 Image analysis of GM1 in rat liver examined at high magnification (40×, NA=0.7). **a** The demonstration of selection of areas in individual measuring frame. Usually several measuring frames are necessary in each field to select 15 areas of sinusoidal membranes and 15 sub-sinusoidal areas of cytoplasm by stratified random sampling method in central zone III and the same was done for neighbouring peripheral areas. **b** GM1 staining in cytoplasm of PD treated rats decreased rapidly in cytoplasm of EE treated rats **c** especially of peripheral zone I. *Bars*=50 µm. Objective magnification in photography 20× (NA=0.5). *CV* = central vein. *PT* = portal area. **d** Linear regression analysis between serum TBA concentration and difference in GM1 ganglioside content between sinusoidal membrane and subsinusoidal area of cytoplasm in zone III. **e** Linear regression analysis between serum TBA concentration and difference in GM1 ganglioside content between sinusoidal membrane and subsinusoidal area of cytoplasm in zone I

activity serves as a marker of purity of canalicular membrane fraction isolated by gradient ultracentrifugation, the changes in ALP activity localization observed in EE-administered rats question the possibility to achieve a satisfactory and reliable purity of membrane fractions. Unlike in normal rat liver, where weak ALP activity was restricted just to the canalicular hepatocyte membrane of peripheral lobular zone, the ALP activity in EE-administered animals was spread over the whole hepatocyte cell membrane except the sinusoidal part in all lobular zones. These results are in agreement with the study showing that the ALP activity in EE-treated rats extends to the central lobular zone [17], whereas a weak activity is confined only to the canalicular hepatocyte membrane at the periphery of the lobule in normal rat [18]. The spreading of ALP from canalicular to lateral membranes explains why ALP is an unreliable marker of canalicular membranes in their isolation from cholestatic livers.

Due to the above mentioned problems in isolation of membranes by ultracentifugation, selective histochemical approach based on specific binding of cholera toxin B-subunit to GM1 was used in our study. The specificity of this binding has been carefully tested on several occasions. Wu and Ledeen [15] confirmed that, among different gangliosides, only GM1 binds cholera toxin B-subunit with very high affinity. In another study, Parton [19] demonstrated that the only components capable of binding cholera toxin B-subunit are glycolipids and not glycoproteins.

To our knowledge, this is the first *in vivo* study demonstrating the localization of gangliosides in normal and cholestatic liver. Our findings in normal rat liver tissue clearly detect GM1 localized on both the canalicular and sinusoidal surfaces of hepatocytes in lobular zones I and II, and its nearly complete absence in liver parenchyma nearby the central vein. In the liver tissue after EE treatment, where the product of histochemical reaction was typically found in all lobular zones, an apparent change of GM1 ganglioside distribution in hepatic lobule was observed. Differences in optical brightness in separate lobular zones III and I, also supported by linear regression analysis, confirmed link between GM1 ganglioside redistribution and cholestasis (Fig. 3). These findings might be associated with lobular blood flow.

As blood flows in liver sinusoids from the periphery to the center of the lobule, numerous substances including bile acids are eliminated by hepatocytes. Considering the well known fact that the higher presence of GSL increases membrane rigidity, we conclude that the shift of GM1 ganglioside localized in the central zone of the liver lobule of EE-treated animals can be a response of the hepatocytes to the harmful effects of bile acids accumulated in sinusoidal blood during cholestasis.

The analysis of gangliosides in liver in EE-induced cholestasis has been described in our previous study [12]. Total lipid sialic acid was almost twice as high as compared to control rats (p=0.002). The TLC analysis of GM1 ganglioside in rat livers showed only slight insignificant increase in EE-treated rats when compared with controls, but gangliosides of *b*-branch of biosynthesis GD3, GD1b and GT1b are increased significantly. In this study we could confirm our previous TLC results that in total liver extract GM1 is not enhanced in EE-treated animals (Fig. 5b). The

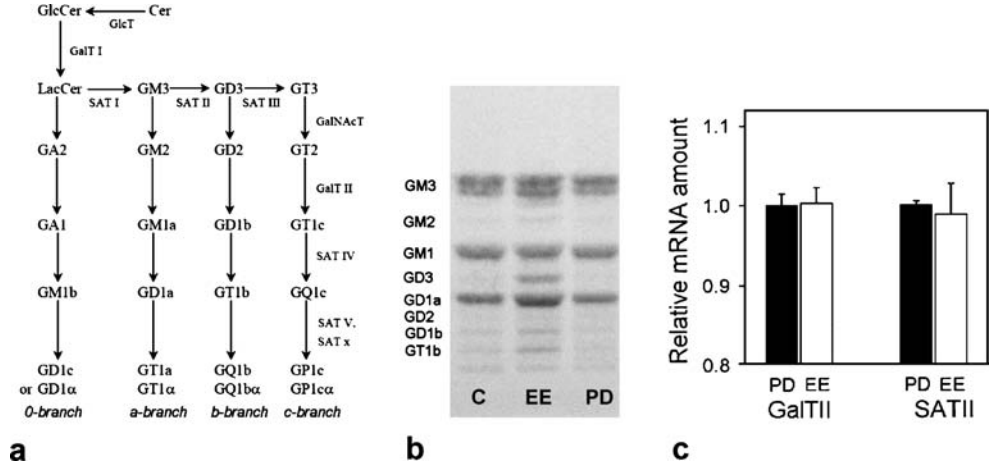

Fig. 5 **a** Scheme of ganglioside biosynthesis with branches *0, a, b* and *c*. Abbreviations of enzymes catalyzing the indicated reactions: *SAT I, II, and III*—sialyl(NeuAc)-transferases I, II, and III; *GalTII*—galactosyl(Gal)-transferase; *GalNAcT*—*N*–acetylgalactosaminyl(GalNAc)-transferase; *SAT IV, V, and X*—sialyl(NeuAc)-transferase IV, V and X. **b** TLC of gangliosides in untreated control (C), EE-treated (EE) and propanediol-treated (PD) rat liver shows an increase in *b*-branch gangliosides and GD1a *a* branch , but GM1 is not significantly increased. **c** Real-time PCR analysis of *GalTII* and *SATII* mRNA in liver cells. Total RNA was isolated from liver cells of control and EE-treated animals and subjected to real-time-PCR using primers for actin, *GalTII* and *SATII*. Results shown are representative of three independent experiments performed in triplicates

data on mRNA analysis of GalTII are in accordance with TLC results. The different distribution of GM1 gangliosides in zones I and III in the EE-treated animals, compared to control samples, and the same level (content) of GM1 and mRNA for GalTII (GM1-synthase) in both groups suggest that not higher biosyntesis in the whole liver but rather locally confined differences in biosynthesis in the central zone might be responsible for the observed differences in increased GM1 expression in sinusoidal surface of central zone in EE-treated animals. It should also be noted that the increase in GD3, observed by TLC does not seem to be due to an increased expression of SATII, as can be inferred from the results of RT-PCR analysis. Further studies, e.g. determination of sialyltransferase activity are necessary for explanation of the increase in *b*-branch gangliosides.

Detailed densitometry at high magnification of the sinusoidal membrane in peripheral zone I did not show any significant increase of GM1 staining in EE-treated animals when compared with those treated with PD or those with no treatment (see data in Table 3b and i). These data suggest that GM1 concentration in sinusoidal membrane in peripheral lobular zone is present to a limited extent even in control animals. It thus seems that hepatocytes in peripheral zone I are attacked by harmful molecules even in untreated animals.

Very surprising is our observation of decreased GM1 staining in subsinusoidal area of peripheral zone cytoplasm. One possible explanation might be that the GM1 is rapidly transported by endosomes from cytoplasm into membranes at limited GM1 biosynthesis. This conclusion is supported by TLC densitometry data [12] and the results of RT-PCR.

The two main findings of densitometric analysis under high magnification, (a) namely the increase of sin/cyt ratio due to increased staining of sinusoidal surface in zone III, and (b) the increase of sin/cyt ratio in zone I due to a decrease in GM1 staining in cytoplasm, correspond with the increased TBA blood concentration in EE-treated animals.

According to previous reports, a shift in lipid content occurs within hepatocyte membranes during cholestasis contributing to the modulation of membrane fluidity [7, 9]. The results of this study prove that GSL redistribution might be responsible for these changes. This conclusion is also corroborated by the known fact that ganglioside molecules are more rigid due to the conformation of ceramide and oligosaccharide parts of the molecule. The ceramide portion adopts a rigid conformation with two closely packed, parallel hydrocarbon chains [20–22], while the oligosaccharide portion is conformationally dependent on the high stability of sialic acid [23] and some other factors [24]. It is well established that the presence of gangliosides reduces the membrane fluidity [25].

Our study documents for the first time that GM1 ganglioside appears in enhanced levels in sinusoidal membranes of hepatocytes during cholestasis. It further demonstrates that microscopic methods remain an important analytical tool, especially in those situations where biochemical and genetical approaches reach their limits.

Acknowledgements We thank Marie Zadinová and Martin Leníček for their help with animal experiments and Alena Veselá and Ladislav Trnka for their excellent technical assistance. This work was supported by the Internal Grant Agency of the Ministry of Health of the Czech Republic, Project No. 8079-3.

References

1. van Meer, G., Lisman, Q.: Sphingolipid transport: rafts and translocators. J. Biol. Chem. **277**, 25855–25858 (2002)
2. Hakomori, S.: Structure, organization, and function of glycosphingolipids in membrane. Curr. Opin. Hematol. **10**, 16–24 (2003)
3. Slimane, T.A., Hoekstra, D.: Sphingolipid trafficking and protein sorting in epithelial cells. FEBS Lett. **529**, 54–59 (2002)
4. van Ijzendoorn, S.C.D., Zegers, M.M.P., Kok, J.W., Hoekstra, D.: Segregation of glucosylceramide and sphingomyelin occurs in the apical to basolateral transcytotic route in HepG2 cells. J. Cell Biol. **137**, 347–357 (1997)
5. Rodriguez-Garay, E.A.: Cholestasis: human disease and experimental animal models. Ann. Hepatol. **2**, 150–158 (2003)
6. Balistreri, W.F., Leslie, M.H., Cooper, R.A.: Increased cholesterol and decreased fluidity of red cell membranes (spur cell anaemia) in progressive intrahepatic cholestasis. Pediatrics **67**, 461–466 (1981)
7. Smith, D.J., Gordon, E.R.: Role of liver plasma membrane fluidity in the pathogenesis of estrogen-induced cholestasis. J. Lab. Clin. Med. **112**, 679–685 (1988)
8. Rosario, J., Sutherland, E., Zaccaro, L., Simon, R.F.: Estradiol administration alters liver sinusoidal membrane fluidity and protein composition. Biochemistry **27**, 3939–3946 (1988)
9. Vu, D.D., Tuchweber, B., Raymond, P., Yousef, I.M.: Tight junction permeability and liver membrane fluidity in lithocholate induced cholestasis. Exp. Mol. Pathol. **57**, 47–61 (1992)
10. Hyogo, H., Tazuma, S., Kajiyama, G.: Transcytotic vesicle fusion is reduced in cholestatic rats: redistribution of phospholipids in the canalicular membrane. Dig. Dis. Sci. **44**, 1662–1668 (1999)
11. Hyogo, H., Tazuma, S., Kajiyama, G.: Biliary excretory function is regulated by canalicular membrane fluidity associated with phospholipid fatty acyl chains in the bilayer: implications for the pathophysiology of cholestasis. J. Gastroenterol. Hepatol. **15**, 887–894 (2000)
12. Majer, F., Trnka, L., Vítek, L., Jirkovská, M., Mareček, Z., Šmíd, F.: Estrogen-induced cholestasis results in a dramatic increase of b-series gangliosides in the rat liver. Biomed. Chromatogr. (accepted for publication)
13. Yu, R.K., Ledeen, R.W.: Gangliosides of human, bovine, and rabbit plasma. J. Lipid Res. **13**, 680–686 (1972)
14. Lojda, Z., Gossrau, R., Schiebler, T.H.: Enzyme Histochemistry. A Laboratory Manual, p. 67, Springer, Berlin Heidelberg New York (1979)
15. Wu, G., Ledeen, R.K.: Quantification of gangliotetraose gangliosides with cholera toxin. Anal. Biochem. **173**, 368–375 (1988)
16. Hamilton, P.W.: Designing a morphometric study. In: Hamilton, P.W., Allen, D.C. (eds) Quantitative Clinical Pathology. Blackwell Science, Cambridge, MA (1995)
17. Arrese, M., Pizzaro, M., Solís, N., Koenig, C., Accatino, L.: Enhanced biliary excretion of canalicular membrane enzymes

in ethinylestradiol-induced cholestasis. Effects of ursodeoxycholic acid administration. Biochem. Pharmacol. **50**, 1223–1232 (1995)
18. Koudstaal, J., Runsink, A.P., van der Sandt, M., Hardonk, M.J.: Correlation between serum alkaline phosphatase and localization of alkaline phosphatase in the liver. Acta Histochem. Suppl. **14**, 129–138 (1975)
19. Parton, R.G.: Ultrastructural localisation of gangliosides. GM1 is localised in caveolae. J. Histochem. Cytochem. **42**, 155–166 (1994)
20. Pascher, I.: Molecular arrangements in sphingolipids. Conformation and hydrogen binding of ceramide and their implication on membrane stability and permeability. Biochim. Biophys. Acta **455**, 433–451 (1976)
21. Harris, P.L., Thornton, E.R.: Carbon-13 and proton nuclear magnetic resonance of gangliosides. J. Am. Chem. Soc. **100**, 6738–6745 (1978)
22. Pascher, I., Lundmark, M., Nyholm, P.G., Sundell, S.: Crystal structures of membrane lipids. Biochim. Biophys. Acta **1113**, 339–373 (1992)
23. Czarniecki, M.F., Thornton, E.R.: Carbon-13 nuclear magnetic resonance spin-lattice relaxation in the N-acylneuraminic acid. Probes for internal dynamics and conformational analysis. J. Am. Chem. Soc. **99**, 8273–8278 (1977)
24. Tettamanti, G., Masserini, M., Giuliani, A., Pagani, A.: Structure and function of gangliosides. Ann 1st Super Sanita **24**, 23–31 (1988)
25. Bertoli, E., Masserini, M., Sonino, S., Ghidoni, R., Cestaro, B., Tettamanti, G.: Electron paramagnetic resonance studies on the fluidity and surface dynamics of egg phosphatidylcholine vesicles containing ganglioside. Biochim. Biophys. Acta **467**, 196–202 (1981)
26. Svennerholm, L.: Chromatographic separation of human brain gangliosides. J Neurochem. **10**, 613–623 (1963)
27. Svennerholm, L.: Designation and schematic structure of gangliosides and allied glycosphingolipids. Prog. Brain Res. **101**, XI–XIV (1994)
28. IUPAC-IUB Commission on Biochemical Nomenclature. The nomenclature of lipids. Recommendations. Lipids **12**, 455–468 (1977)